Journal of Materials Chemistry B

Accepted Manuscript

ROYAL SOCIETY OF CHEMISTRY

www.rsc.org/materialsB

Docetaxel-loaded PEO–PPO–PCL/TPGS mixed micelles for overcoming multidrug resistance and enhancing antitumor efficacy

Chunhuan Shi[a], Zhiqing Zhang[b], Fang Wang[b], Xiaoqing Ji[a], Zhongxi Zhao[a] and Yuxia Luan[a]*

[a] *School of Pharmaceutical Science, Shandong University, 44 West Wenhua Road, Jinan, Shandong Province, 250012, P. R. China. Fax: (86) 531-88382548; Tel: (86) 531-88382007; E-mail: yuxialuan@sdu.edu.cn*

[b] *College of Science, China University of Petroleum, 66 West Changjiang Road, Qingdao, Shandong 266580, P. R. China.*

Abstract:

There are two major hurdles for the currently anti-cancer drug delivery systems. One is the emergence of multidrug resistance (MDR) and the other is the conflict between long-circulation and cellular uptake. In present study, the anticancer drug docetaxel (DTX) was successfully loaded into three series of micelles via self-assembly using a mixture of PEO–PPO–PCL and D-α-tocopheryl poly (ethylene glycol) 1000 succinate (TPGS), for the purpose of prolonging the blood circulation time as well as overcoming MDR of DTX. Three series of copolymers with different PCL molecular weight, PEO_{68}-PPO_{34}-PCL_{9}, PEO_{68}-PPO_{34}-PCL_{18} and PEO_{68}-PPO_{34}-PCL_{36} were synthesized. The prepared spherical mixed micelles (MM) were found to possess nanoscale size (25 nm - 135 nm). The PEO–PPO–PCL/TPGS mixed micelles had low critical micelle concentration (~10^{-6} g mL^{-1}) and low hemolysis rate (<5%), which has proved they were safe for use *in vivo*. Moreover, they had obvious sustained release behavior *in vitro* and longer circulation time than free DTX *in vivo*. The P-gp inhibition assay, cellular uptake and MTT assay in cancer cells exhibited that DTX-loaded MM could overcome MDR, get higher cellular uptake and higher antitumor efficacy than free DTX. The IC50 values demonstrated that the three series DTX-loaded MM were 69, 82 and 100 folds effective than free DTX after 72 h treatment with MCF-7 cells, respectively. Therefore, these results demonstrated that the prepared DTX-loaded MM provide desirable application for cancer chemotherapy.

KEYWORDS: PEO-PPO-PCL, TPGS, docetaxel, micelles, multidrug resistance

1. Introduction

Cancer is still one of major causes of death worldwide and chemotherapy is currently a predominant but far from satisfying method to treat cancer because of the emergence of multidrug resistance (MDR).[1] The most extensively studied mechanism of MDR is the overexpression of ABC-transporter P-glycoprotein (P-gp), which can purge a wide range of drugs from cells and thereby decreasing their intracellular accumulation in drug-resistant cells.[2]

It is well acknowledged that docetaxel (DTX) is an important anticancer taxane which has been used with success in patients with various human malignancies. However, like many other classic chemotherapeutic agents, DTX also has solubility issues in water due to the bulky polycyclic structure (Scheme 1). Low solubility leads to short blood circulation time in body, erratic absorption patterns and frequent administrations, which detracts from the clinical potency of the drugs. What's worse, the potential effects are undermined by the presence of MDR. Additionally, the clinical formulation Duopafei® has been found to evoke serious side effects due to the nonionic surfactant Tween-80 or ethanol in saline solution.[3,4] These shortcomings of DTX have considerably impeded its clinical use. Therefore, the new formulation is urgent to improve the solubility of DTX as well as to avoid the MDR and minimize undesirable side-effects.

Nanotechnology is a viable and versatile strategy for the efficacy of chemotherapeutic agents.[5] As one of the representative nanocarriers, polymeric micelles have sparked a considerable interest because of their technical simplicity and prominent superiorities, such as the high stability, prolonged systemic circulation, ease of active targeting modification, the great flexibility in tuning drug solubility and so on.[6-8] Polymeric micelles can be self-assembled from amphiphilic polymers in aqueous media, characterized by a typical core-shell structure, which can efficiently encapsulate hydrophobic anticancer drugs.[9-13] Compared with singular copolymer micelles, mixed micelles have more prominent advantages, such as enhancing drug loading capacities, significant improvements in thermodynamic, improving kinetic stability, increasing cellular uptake and so on. Multiple functional micelles can be designed by rational combination of different copolymers or by incorporating

functional substances into the micelles.[14-17] It is a convenient approach to integrate multiple functions in one system without complicated synthetic schemes.

In our previous work, the amphiphilic triblock copolymers of poly (ethylene oxide)-block–poly (propylene oxide)-block–poly (ε-caprolactone) (PEO–PPO–PCL) with various block compositions have been synthesized by ring-opening polymerization (ROP) of ε-caprolactone (ε-CL) initiated by the OH group of methoxy–poly (ethylene oxide)–poly (propylene oxide) (Me–PEO–PPO).[18] The molecular weights of the PEO and PPO segments were fixed, while the length of the PCL copolymer chains was different. Herein we obtained three series of copolymer, PEO_{68}-PPO_{34}-PCL_9, PEO_{68}-PPO_{34}-PCL_{18} and PEO_{68}-PPO_{34}-PCL_{36}, named by P9, P18, and P36, respectively, wherein the digits after P represent the degree of polymerization of PCL. The synthesized three copolymers have particular potential for biomedical use in drug delivery systems. A prominent feature of the PEO–PPO–PCL copolymer is the ability to self-assemble into polymeric micelles at low critical micelle concentration (CMC) in aqueous solutions. In the copolymers, the flexible EO chain is the hydrophilic part, which serves as the outer corona and is stealthy to immune system,[19] whereas the PO and CL chains can serve as a cargo space for hydrophobic drug.

It is known that DTX can be pumped out of the cell by P-gp and fail to accumulate to cytotoxic levels. The designed mixed micelles in present study aim to improve the cellular uptake by bypass the P-gp efflux pumps (DTX incorporation into micelles) and inhibition the P-gp efflux pumps (addtion of P-gp inhibitor). Thus, co-administration of P-gp inhibitors is also an important aspect in this study. However, some small molecules (e.g. verapamil and cyclosporin A) require high concentrations for their inhibitory activity and always induce unwanted effects. D-α-tocopheryl polyethylene glycol 1000 succinate (TPGS) has been approved as a safe pharmaceutical adjuvant in drug delivery system and widely used as P-gp inhibitor in overcoming MDR.[20,21] It is an amphiphilic molecule and formed by esterification of Vitamin E succinate with polyethylene glycol (PEG) 1000 (Scheme 1). It can self-assemble into micelles in the aqueous solution. TPGS is usually mixed with other materials to prepare mixed micelles. Therefore, TPGS used in combination with PEO-PPO-PCL to form mixed micelles to overcome MDR is a better choice. Moreover,

compared to the singular PEO-PPO-PCL micelles, the addition of TPGS is expected to increase the drug loading and improve micelles stability due to the increased inner micelle core volume through the big vitamin E head.[22] It is reported that TPGS can achieve synergistic effects with the anticancer drug and the anticancer efficacy of TPGS is associated with its increasing ability to induce cell apoptosis in the presence of anticancer agent.[23] Therefore, TPGS, as a constituent of mixed micelles, can bring many advantages to the micelle system and improve the therapeutic efficacy of cancer treatments.

In present work, we construct drug delivery systems comprised of synthesized PEO-PPO-PCL copolymers and TPGS for increasing DTX's anti-tumor activity, in which TPGS is designated as a component to increase the drug loading and an inhibitor of the MDR efflux pump. The DTX-loaded PEO-PPO-PCL/TPGS mixed micelles can have a combined effect as a nanocarrier, P-gp inhibitor, and anticancer efficacy enhancer. Here, we describe the preparation of MM and their physicochemical characterizations. Moreover, the drug delivery system was evaluated *in vivo* pharmacokinetics and *in vitro* release behavior, cellular uptake and cytotoxicity. The results demonstrate that the mixed micelles can well control the drug release behavior, overcome MDR and enhance the antitumor activity of DTX. Thus, the prepared mixed micelles may be a promising platform for enhancing the therapeutic efficacy of drugs.

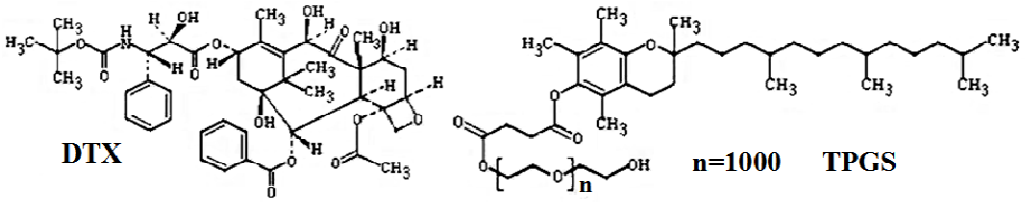

Scheme 1. The chemical structures of DTX and TPGS.

2. Experimental

2.1 Materials

Docetaxel and verapamil hydrochloride (Vrp·CL) were purchased from Dalian Meilun Biotech Co., Ltd. D-α-tocopheryl polyethylene glycol 1000 succinate (TPGS) was purchased from Aladdin (China). 3-(4,5-Dimethylthiazol-2-yl)-2,5-diphenyl

tetrazolium bromide (MTT), propidium iodide (PI), rhodamine 123, coumarin-6 and dimethyl sulphoxide (DMSO) were purchased from Sigma-Aldrich (China). Cellulose ester membranes (diaysis bag) with a molecular weight cut-off value (MWCO) of 3500 (Greenbird Inc., Shanghai, China) were used in dialysis study. PEO–PPO–PCL were synthesized a method described previously.[18] RPMI (Roswell Park Memorial Institute) 1640, fetal bovine serum, 0.25% (w/v) trypsin–0.03% (w/v) EDTA, plastic cell culture dishes and plates were purchased from Gibco BRL (Gaithersberg, MD, USA). Water used in the experiment was doubly distilled and deionized. The acetonitrile (Shanghai Siyou Co., Ltd., China) was HPLC grade. All other solvents were analytical- or chromatographic-grade.

2.2 ^{1}H NMR analysis of copolymer and GPC measurements. The ^{1}H NMR spectra of the copolymers were recorded on a Varian Mercury Plus-400 NMR spectrometer (Varian, USA) operating at 400 MHz with $CDCl_3$ as a solvent.

The molecular weights of PEO-PPO-PCL were determined by gel permeation chromatography (GPC; Wyatt Technology). GPC analyses were performed in THF, using monodispersed polystyrene standards for calibration.

2.3 Preparation of mixed micelles. DTX-loaded MM was prepared by thin film hydration method. The optimum preparation condition is firstly selected by means of orthogonal test designs. Firstly, DTX (10 mg), PEO-PPO-PCL (160 mg) and TPGS (40 mg) were co-dissolved in acetonitrile to form a homogeneous polymeric matrix. Then, the solution was evaporated on a rotary evaporator under reduced pressure at 40 °C to form a thin film. This film was further dried under high vacuum 24 h to remove any traces of remaining solvent, and then hydrated with water (5 mL), incubated at 60 °C for 1 h, and then sonicated for 10 min. Finally, the resultant mixture was filtered through 0.22 μm polyethersulfone syringe filter in a sterile and the MM was successfully prepared. The blank MM was prepared as the same method as above except that the DTX was not added.

2.4 Characterization of DTX-loaded mixed micelles. The average size and size distribution of the micelles were measured by dynamic light scattering method (DLS) from the signal intensity using Delsa™ Nano Submicron Partie Size Analyzer (A53878). The zeta potential of the micelles was also measured using the same

instrument. Each sample was run for 3 times with 1 min duration. The samples were diluted with tri-distilled water to 5 mg/mL.

The morphology of polymeric micelles was examined by transmission electron microscopy (TEM, JEM-200CX). Samples were prepared by placing a drop of freshly prepared suspension onto a 300-mesh copper grid. Copper grids were surface-coated to form a thin layer of amorphous carbon.[24] Then negatively stained with 2% (w/v) phosphotungstic acid for 30 s. Air-dried samples for 10 min at room temperature were observed.

The amount of DTX encapsulated in the mixed micelles was measured by high performance liquid chromatography (HPLC, Agilent LC1100). Mobile phase was a mixture of acetonitrile and water (65:35, v/v) and the flow rate of mobile phase was 1 mL/min. The column effluent was detected at 230 nm with a UV/VIS detector. Drug loading (DL %) and encapsulation efficiency (EE %) were calculated by the following equations:

$$\text{DL}\ (\%) = \frac{\text{Weight of DTX in MM}}{\text{Weight of MM}} \times 100\%$$

$$\text{EE}\ (\%) = \frac{\text{Weight of DTX in MM}}{\text{Weight of feeding DTX}} \times 100\%$$

2.5 Critical micelles concentration of mixed micelles. The critical micelles concentration (CMC) was determined by the fluorescence probe technique using pyrene as a fluorescence probe.[25] Aliquots of pyrene solution (30×10^{-6} M in acetone, 0.1 mL) were added to 10 mL flask and the acetone was allowed to evaporate to form a thin film. Then a series of stock micelles solution ranging from 0.2 to 30 μg/L were added into the flasks and the final concentration of pyrene was 6×10^{-7} M in the solution. The polarity of the microenvironment surrounding pyrene was estimated by examining the I_{373}/I_{384} nm vibronic band ratio of the fluorescence spectrum. Excitation wavelength was 334 nm. Spectra were recorded ranging from 350 to 450 nm.

2.6. Micelle stability

2.6.1 Storage stability. DTX-loaded MM were stored at 4 ◦C for 3 months. The physical stability of micelles was evaluated by monitoring the time-dependent

changes in the physical characteristics (drug precipitation, change in micelle size/size distribution) of the formulation.

2.6.2 The stability in media modeling physiological conditions. To examine the stability in the blood serum, the DTX-loaded MM were suspended in PBS solution (pH 7.4) containing 10% fetal bovine serum (FBS) and incubated for 72 h at 37 °C. The stability was evaluated by monitoring the time-dependent changes in micelle size by DLS.[26]

2.7 In vitro drug release studies. 0.5 mL DTX-loaded micelles or free DTX solution (with an equivalent DTX concentration of 0.5 mg mL^{-1}) was placed in a dialysis bag (molecular mass cut-off 3500 Da). The dialysis bags were incubated in 20 mL of PBS buffer (pH 7.4) containing 0.1% w/v Tween-80 at 37 °C with horizontally shaking (120 rpm/min). Herein, Tween-80 was used to improve the solubility of DTX in PBS. If Tween-80 was not used in the drug release studies, DTX would not be further released when the concentration reached its saturated concentration in PBS. At predetermined time intervals, 1 mL of the incubation medium was removed, and the same volume of fresh solution was added. The amount of DTX released at each time point was determined by HPLC as described in section 2.4. The measurement was performed in triplicate.

2.8 Hemolytic evaluation. To ensure the micelles are safe to be intravenous injected. The hemolytic potential of the DTX-loaded MM is essential to be investigated. Hemolytic study was performed following the previously reported procedure with minor modifications.[27] Briefly, 1.0 mL RBC suspension (2% w/v) was dispersed in 4.0 mL distilled water and 4.0 mL normal saline as positive control and negative control, respectively. 1.0 mL mixed micelles solutions with different concentrations added to 3.0 mL of normal saline and interacted with 1.0 mL RBC suspension. All of the samples were incubated in a 37 °C water bath for 2 h and then centrifuged at 3000 rpm for 10 min. Then 100 μL of supernatant of each sample was transferred to a 96-well plate. The absorbance was determined at 540 nm with a microplate reader (Bio-Rad Laboratories, Hercules, CA, USA). The degree of hemolysis was determined by the following equation:

$\text{Hemolysis}(\%) = \frac{A_{\text{sample}} - A_{\text{negtive}}}{A_{\text{positive}} - A_{\text{negtive}}} \times 100\%$. When this value was greater than 5%, the sample possessed hemolytic potential.

2.9 In vivo pharmacokinetics study

2.9.1 Animals. All animal experiments were approved by the Institutional Animal Care and Use Committee of Shandong University and in full compliance with international ethics guidelines. Male wistar rats (200 ± 20 g) were bought from the Experimental Animal Center of Shandong University. They were allowed free access to food and water.

2.9.2 Pharmacokinetics study. The pharmacokinetic of the DTX-loaded MM was investigated to compare free DTX after administration a single 13 mg kg^{-1} dose of DTX via the tail-vein. Blood samples of 0.5 mL were collected from the right jugular vein at 0.08, 0.25, 0.5, 1, 2, 4, 6, 8, 12 and 24 h intervals. Plasma was obtained from whole blood by centrifugation at 5000 rpm for 10 min and stored at −20 °C until analysis. The levels of DTX in the plasma samples were determined by HPLC. All data were measured at least in triplicate.

2.10 *In viro* cells experiments

2.10.1 Cell lines and cell culture. MCF-7/Adr, MCF-7 and A549 cells were kindly donated by the Department of Pharmacology, School of Pharandmacy, Shandong University. The cell culture is given in Supporting Information.

2.10.2 Inhibition of P-gp efflux test in MCF -7/Adr cells. To evaluate the potential P-gp inhibitory effects, P-gp mediated efflux inhibitory trials were carried out on P-gp overexpressing MCF-7/Adr cells. Verapamil (Vrp) was used as a standard P-gp inhibitor. Rhodamine123 (RH123) is a substrate for P-gp and can be used as a marker for P-gp activity in cells. Briefly, MCF-7/Adr cells were cultured with fresh media containing series of treatment samples including Vrp, TPGS, TPGS-micelles, non-TPGS-micelles for 24 h on a 6-well cell culture plate (1×10^5 cells/well). Herein, the untreated cells and cells treated with Vrp were used as the negative control and positive control, respectively. Then RH123 (5 μM mL^{-1}) were put into the wells, after 4 h incubation, the cells were washed twice with cold PBS and visualized by inverted fluorescence microscope (Olympus, Tokyo, Japan).

As for quantitative assessment, cells treated as described above were seeded on a 96-well cell culture plate (5000 cells/well) for 24 h. Finally, cells were washed twice with PBS, and immersed in 50 μL 0.2 g L^{-1} NaOH solutions (containing 0.5% Triton X-100). After 15 min incubation with gentle shaking, the fluorescent intensities were measured with a microplate reader at 430/485 nm (Excitation/Emission).

2.10.3 The cellular uptake of C6-loaded TPGS-micelles and non-TPGS micelles in MCF -7/Adr cells. P-gp overexpressed MCF -7/Adr cells, in which P-gp was much more active, were chosen to test the effect of TPGS on the cellular uptake. Hydrophobic fluorescent dye coumarin-6 (C6) was used as a probe to substitute DTX. C6 was incorporated into the formulations as the same procedure described in Section 2.3. MCF-7/Adr cells were seeded into six-well culture plates (1×10^5 cells/well) and incubated for 24 h. The cells were then incubated at 37 □ with C6-loaded TPGS-micelles and non-TPGS micelles (C6 concentration was 5 μg mL^{-1}). The control is the C6-loaded non-TPGS micelles group. After exposure for 8 h, the cells were washed with cold PBS for three times to remove extracellular C6 and visualized by reverse fluorescence microscopy (Olympus, Japan).

2.10.4 The cellular uptake studies and flow cytometric (FCM) analysis. Cellular uptake of the C6-loaded mixed micelles by MCF-7 and A549 cells were assessed both qualitatively and quantitatively, compared with free C6. The cellular uptake and flow cytometric (FCM) analysis methods are given in Supporting Information. The cells were cultured with free C6 and C6-loaded MM for 2 and 4 h, respectively and then imaged for qualitative experiments. Flow cytometry was utilized to quantify the fluorescence intensity in the cells of 4 h incubation.

2.10.5 Cytotoxicity assay. The cytotoxicity of each sample was determined by MTT assay. MTT assay is described in Supporting Information. Blank micelles, DTX-loaded micelles and free DTX are characterized. Results were presented as cell inhibitory rate and IC50 values, IC50 values (μg mL^{-1}) were calculated using SPSS 17.0 (IBM, USA). Cell inhibitory rate = $(A570_{control} - A570_{sample})/A570_{control} \times 100\%$, where untreated cells were tested as controls.

2.10.6 Drug induced morphology changes and propidium iodide (PI) staining. Drug induced morphology changes and cell membrane integrity changes in MCF-7 and A549 cells were further evaluated. The morphology was observed by reverse

fluorescence microscopy (Olympus, Japan). Propidium iodide (PI), a red-fluorescent, is commonly used for determining the cell membrane integrity. The PI staining process is given in Supporting Information.

2.11 Statistical analysis. All results were expressed as the mean ± standard deviation (SD) unless otherwise noted. Student's t-tests was performed to evaluate the significance of differences between groups considered as Δ $P < 0.05$, * $P < 0.01$.

3. Results and discussion

3.1 ^{1}H NMR and GPC analysis of copolymers. The series of copolymers PEO–PPO–PCL have been synthesized by the successive ring-opening polymerization (ROP) of ε-caprolactone (ε-CL) initiated by the OH group of methoxy–poly (ethylene oxide)–poly (propylene oxide) (Me–PEO–PPO) in our previous work.[18] The ^{1}H NMR spectra of PEO_{68}-PPO_{34}-PCL_9, PEO_{68}-PPO_{34}-PCL_{18} and PEO_{68}-PPO_{34}-PCL_{36} were illustrated in Fig. 1, respectively. The sharp peak at 3.65 ppm is attributed to methylene protons of OCH_2CH_2O in PEO unit. The double peaks at 1.14 ppm, 3.39 ppm, and 3.55 ppm belongs to protons of CH_3, CH, and CH_2 in PPO unit, respectively. Peaks at 1.61 ppm, 2.33 ppm, and 4.06 ppm are assigned to methylene protons of $(CH_2)_3$, $OCCH_2$ and CH_2OOC in PCL blocks, respectively. The peaks between 1.2 ppm to 1.5 ppm belong to water peaks in $CDCl_3$.

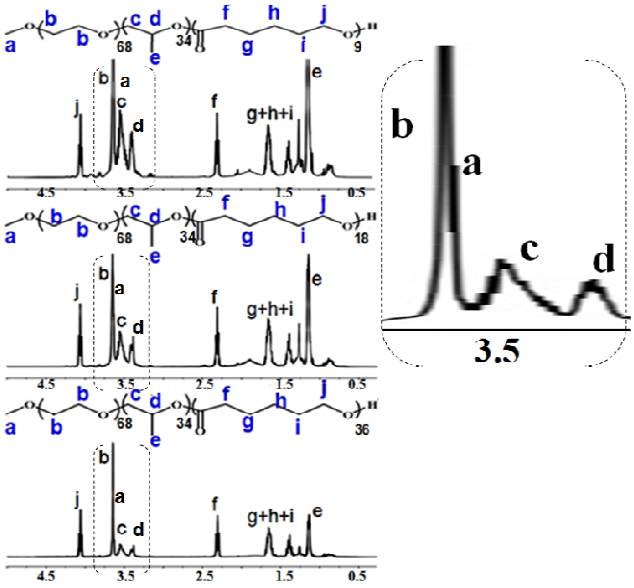

Fig. 1. ^{1}H NMR spectra of copolymer PEO_{68}-PPO_{34}-PCL_9, PEO_{68}-PPO_{34}-PCL_{18} and PEO_{68}-PPO_{34}-PCL_{36} (solvent: $CDCl_3$).

The molecular weight of the three copolymers and corresponding molecular weight distribution were also characterized by GPC. As can be seen from Table 1, those polymers with different molecular weight exhibited a narrow molecular weight distribution as evinced by PDI (1.0-1.3)

Table 1. GPC data of copolymer PEO-PPO-CL

copolymer	Mn	Mw	Mw/Mn (PDI)
PEO_{68}-PPO_{34}-PCL_{9}	4815	6431	1.3
PEO_{68}-PPO_{34}-PCL_{18}	5347	6609	1.2
PEO_{68}-PPO_{34}-PCL_{36}	8995	8996	1.0

3.2 Size, size distribution and morphology of mixed micelles. The blank MM and DTX-loaded MM were prepared respectively. The size and size distribution of micelles are the crucial parameters in the design of drug delivery system, which largely influence the drug release behavior, cellular uptake as well as the *in vivo* pharmacokinetics and biodistribution.[28] The size was measured by dynamic light scattering (DLS) and the results were shown in Fig. 2 and Table 2. The sizes of the blank MM were 23.8 ± 0.7 nm, 33.9 ± 0.6 nm and 132.9 ± 1.1 nm for P9/TPGS, P18/TPGS and P36/TPGS MM, respectively. While, the sizes of DTX-loaded MM were slightly larger than those of corresponding blank MM, they were 25.9 ± 0.5 nm, 35.6 ± 0.4 nm, and 137.2 ± 0.8 nm, respectively. Overall, the size increased with the increase of PCL block length for both blank MM and DTX-loaded MM. The size of micelle is dependent on several factors including relative proportion of hydrophobic and hydrophilic blocks, copolymer molecular weight and micelle aggregation number.[29] In this study, the size of the mixed micelle increases with the increase of hydrophobic blocks, when hydrophilic block is the same. It also could be seen that both blank MM and DTX-loaded MM had narrow size distribution (PDI: 0.17-0.27). It has been reported that particles of between 10 and 200 nm diameter are effective in avoiding the first-pass elimination via glomerular filtration in the kidneys and can escape reticuloendothelial uptake. Furthermore, particles in this size range can be selectively taken up by tumors because of the higher vascular permeability of these cells compared to normal tissue.[30-32] Hence, all the prepared micelles have the desired sizes, falling within the optimum particle size range of 20-200 nm for prolonged

circulation, accumulation in tumor tissue, enhanced diffusion within tissue and uptake by cancer cells.

The TEM images (Fig. 2) showed that the morphology of all the samples was homogeneous spherical nanostructures. It should notice that the diameters of all MM slightly smaller to those obtained by DLS. This was mainly attributed to the dehydration of micelles in the TEM samples preparation process, while the size measured by DLS was in hydrated state.

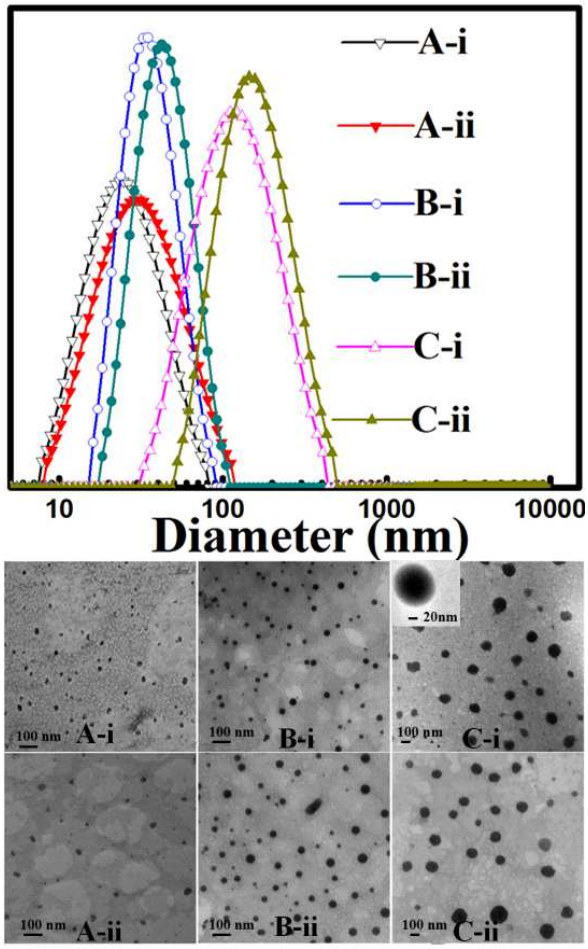

Fig. 2. The DLS and TEM imaging of unloaded (i) and DTX-loaded (ii) (A) P9/TPGS MM, (B) P18/TPGS MM, (C) P36/TPGS MM.

Table 2.

The size and PDI of unloaded (i) and DTX-loaded (ii) (A) P9/TPGS MM, (B) P18/TPGS MM, (C) P36/TPGS MM (mean ± SD, n=3).

Formulations	A-i	A-ii	B-i	B-ii	C-i	C-ii
Size (nm)	23.8 ± 0.7	25.9 ± 0.5	33.9 ± 0.6	35.6 ± 0.4	132.9 ± 1.1	137.2 ± 0.8
PDI	0.26 ± 0.02	0.27 ± 0.04	0.15± 0.03	0.16 ± 0.01	0.23 ± 0.03	0.21 ± 0.05

3.3 Drug loading, encapsulation efficiency and zeta potential. The drug loading (DL), encapsulation efficiency (EE) and zeta potential were investigated. As shown in Table 3, both the DL and EE increased with the increase of PCL block. This can be easily understood because PCL block form the hydrophobic core of the micelles. The longer the hydrophobic block is, the larger the core size and thus the greater ability to entrap hydrophobic drugs. Zeta potential is an indicator of the surface charge. The zeta potentials of all samples were slightly negative, about -0.3 mV. Previous studies have demonstrated that the negatively and neutral charged aggregates can avoid the strong forces with serum proteins and macrophage uptake in the circulation system. In contrast, the aggregates with positively charge would be rapidly cleared from the circulation system.[33,34] Thus, the mixed micelles we prepared could exhibit higher colloidal stability and longer circulation time than positively charged aggregates.

It also could be observed that the PEO-PPO-PCL/TPGS MM have higher loading capacity compared to the corresponding single PEO-PPO-PCL micelles. The reason was that the TPGS comprises a lipophilic head portion and the bulky lipophilic aromatic ring which can make the polymeric micelle hydrophobic core larger, thereby allowing for more DTX molecules to be encapsulated.

Table 3.

The drug loading (DL), encapsulation efficiency (EE) and zeta potential of MM (mean ± SD, n=3).

Formulations	DL (%)	EE (%)	Zeta potential (mV)
DTX-loaded P9	1.91 ± 0.02	40.11 ± 0.42	-0.33 ± 0.07
DTX-loaded P18	3.02 ± 0.03	63.42 ± 0.86	-0.27 ± 0.11
DTX-loaded P36	3.52 ± 0.03	75.39 ± 0.74	-0.25 ± 0.02
DTX-loaded P9/TPGS	2.48 ± 0.02	50.94 ± 0.98	-0.39 ± 0.12
DTX-loadedP18/TPGS	3.47 ± 0.04	71.92 ± 0.49	-0.28 ± 0.12
DTX-loaded P36/TPGS	4.40 ± 0.03	92.07 ± 0.86	-0.23 ± 0.08

3.4 Critical micelles concentration of mixed micelles. CMC is an important parameter for indicating the stability of micelles, both *in vitro* and *in vivo*. Pyrene has been widely used to estimate the polarity of the environment where it locates as well as the CMC of amphiphiles using the intensity ratio of the first and third vibronic peaks, I_1/I_3. As shown in Fig. 3 (I- III), the fluorescence intensity increased as concentration of the polymer increased.[35] The CMC was found to decrease upon the increase in the length of the hydrophobic block, because the higher hydrophobicity renders the formed micelles more compact. The CMC of P9/TPGS MM, P18/TPGS MM and P36/TPGS MM (Fig. 3 IV) were 3.6, 1.5 and 0.7 mg L^{-1}, respectively, lower than those of corresponding PEO-PPO-PCL MM,[18] which endowed a higher stability and ability to maintain the integrity even upon strong dilution in the body.

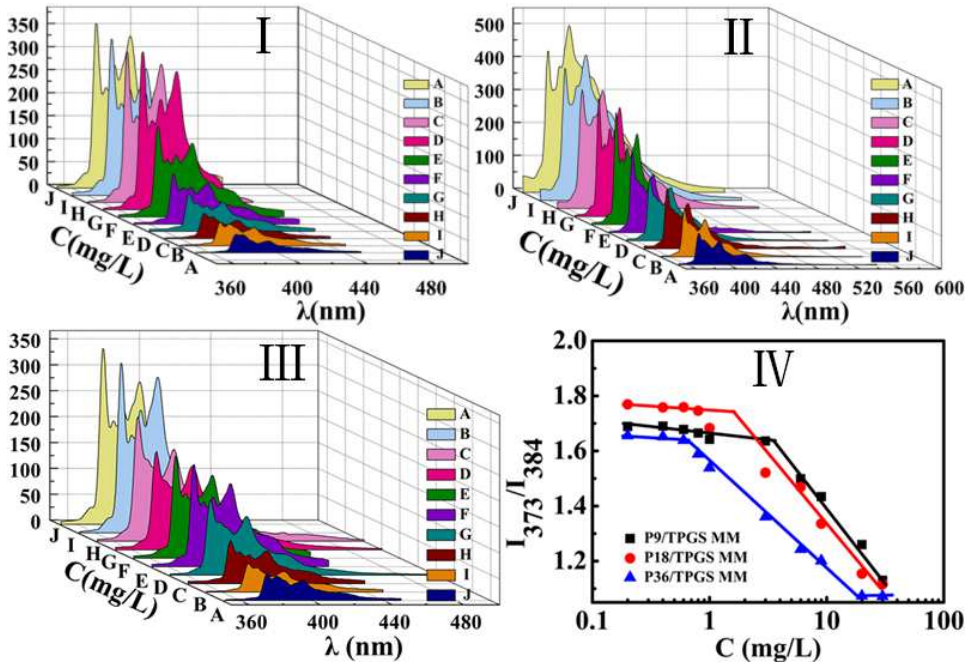

Fig. 3. (I- III) Fluorescence spectra of pyrene in the P9/TPGS MM, P18/TPGS MM and P36/TPGS MM solution. (A) 0.2, (B) 0.4, (C) 0.6, (D) 0.8, (E) 1, (F) 3, (G) 6, (H) 9, (I) 20, (J) 30 mg L^{-1}. (IV) Intensity ratio (I_{373}/I_{384}) of pyrene as a function of polymer concentration.

3.5. Micelle stability

3.5.1 Storage stability. The DTX-loaded MM were stable during storage at 4 ◦C for 3 months. When visually inspected (Fig. 4 I), no phase separation and precipitation were occurred after 3 months. As illustrated in Fig. 4 II, the size and size distribution (PDI) of DTX-loaded MM was fairly stable when stored at 4 °C for a period of 3 months. By DLS, there were also no obvious intensity changes during this time (Table S1). Thus, all the mixed micelles were able to retain drugs co-encapsulated in the system over this period.

3.5.2 The stability in media modeling physiological conditions. Considering their future *in vivo* application, the DTX-loaded MM should be stable at physiological conditions (PBS 7.4, with 10% FBS at 37 °C). As revealed in Fig. 4 III, the micelles did not show significant change in size or size distribution (PDI) over 72 h incubation in a serum-containing medium at 37 °C, which indicated that no adsorption of serum proteins on the micelle corona occurred. It also can be seen from Fig. 4 (II) and (III) that FBS has no effect on the size of DTX-loaded mixed micelle. The good stability

was mainly caused by the importance of the PEO chain to maintain the steric hindrance and largely avoided interactions with serum proteins by the production of a hydrophilic shell layer.[36]

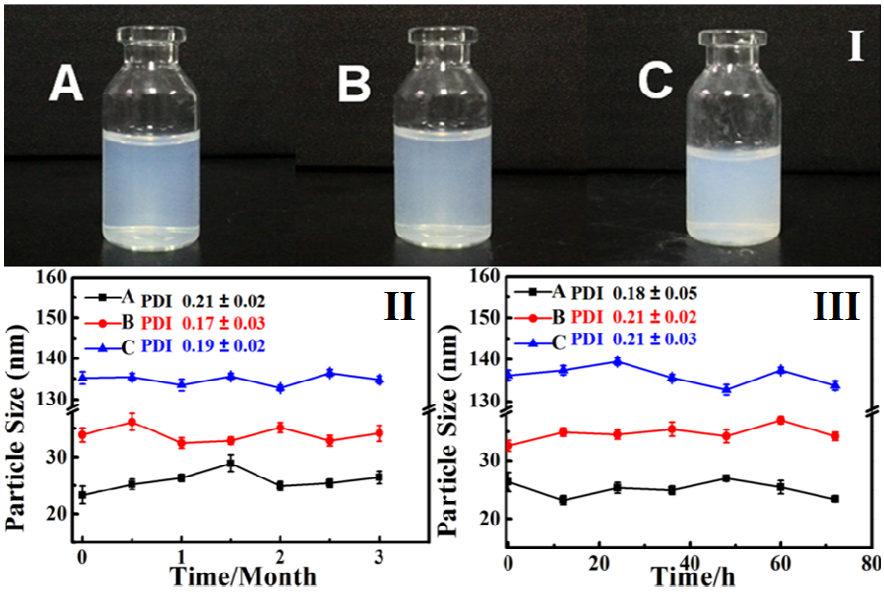

Fig. 4. (I) Photographs of the DTX-loaded MM stored at 4 °C after 3 months. (II) The size of the DTX-loaded MM stored at 4 °C for 3 months. (III) The size of the DTX-loaded MM stored in the presence of FBS at 37 °C for 72 h. (A) DTX-loaded P9/TPGS MM, (B) DTX-loaded P18/TPGS MM, (C) DTX-loaded P36/TPGS MM.

3.6 In vitro drug release studies. Sustained release of drug from nanoparticles represents another important characteristic for a drug delivery system. The *in vitro* release behavior of DTX presented as the accumulative percentage release was shown in Fig. 4. The pH 7.4 PBS solution here was selected to simulate the environment of blood and free DTX was investigated as a control. It was found that about 100% of free DTX was released after approximately 12 hours. While, the DTX released amounts reached about 41%, 56% and 58% for P9/TPGS MM, P18/TPGS MM and P36/TPGS MM, respectively, in the same periods. Obviously, the release of free DTX was much faster than those from three DTX-loaded MM. This was because free DTX could freely diffuse through the dialysis membrane, while encapsulated DTX firstly needed to be released from the micelles and then diffused out of the dialysis bag. For the three DTX-loaded MM, the release rate decreased as the increase of the molecular weight of the PCL block. DTX-loaded P36/TPGS MM reached a plateau in 72 h with approximately 79% DTX released. For P9/TPGS MM and P18/TPGS MM, the

release rate was too slow to be detected after 48 h and the release amount was found to be 76% and 77%, respectively. DTX is an aqueous poor soluble substance and encapsulated into the hydrophobic core of the micelle. The release behavior of drug from the core–shell structure micelles was largely dependent on the hydrophobic interaction between the inner core and drug. It has been reported that the interaction between drug and core was increased with the larger hydrophobic block of the copolymer and the entrapped drug would take relatively long time to diffuse across the polymer micelle to the medium due to strong hydrophobic interaction.[38] Therefore, in the present study the release rate of P36/TPGS is much slower compared to that of P18/TPGS and P9/TPGS. In addition, the three series carriers contained the equal amounts of DTX, thus the close release amount were obtained in the end.

All the release profiles (Fig. 5) have shown initial burst from micelles in the first few hours, which was reasonably controlled by diffusion of DTX molecules located at the region near or within the PEO shells.[37] Subsequently, DTX encapsulated inside the core released sustainably. Due to a limited DTX burst of three types of micelles and the slower drug release rate, it was conceivable that a large amount of DTX would be retained in the core during micelle circulation in the bloodstream under physiological conditions.

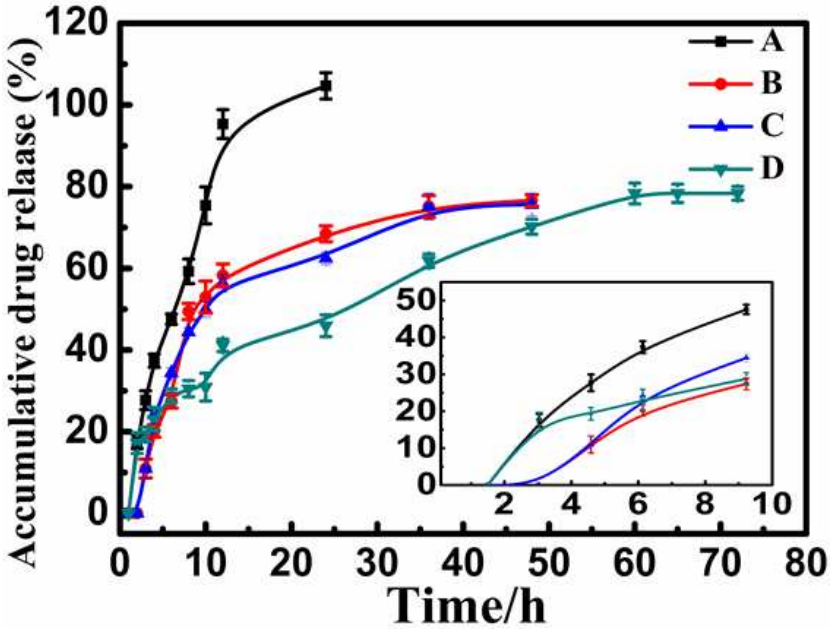

Fig. 5. In vitro release curves of DTX from (A) free DTX, (B) DTX-loaded P9/TPGS MM, (C) DTX-loaded P18/TPGS MM, (D) DTX-loaded P36/TPGS MM (mean ± SD, n=3).

3.7 Hemolytic evaluation. Hemolytic evaluation could give additional information about the biocompatibility of the MM in the case of *in vivo* application. The hemolytic potential of the three MM was shown in Table 4. The hemolytic rate of all these micelles were under 5%, indicating that the hemolysis was not evident and the micelles were safe for i.v. administration.[38] The low hemolytic activity should be originated from the negatively charged surface, and the protective layer of MM formed by PEO segments. Moreover, negligible hemolytic activity also gave the general indication that the micelles did not significantly disassemble into unimers, which was the main responsible for hemolysis.

Table 4

The hemolysis (%) of the DTX-loaded MM at different concentrations (mean ± SD, n=3).

Formulations	Concentration (mg mL^{-1})				
	0.02	0.20	2.00	20.00	40.00
DTX-loaded P9/TPGS	1.53 ± 0.31	2.51 ± 1.85	2.43 ± 1.63	3.56 ± 0.13	1.86 ± 0.96
DTX-loaded P18/TPGS	3.90 ± 0.21	2.33 ± 1.39	4.23 ± 0.88	0.84 ± 0.92	0.96 ± 0.69
DTX-loaded P36/TPGS	3.13 ± 0.34	1.27 ± 0.96	2.56 ± 1.20	4.14 ± 0.62	1.07 ± 0.37

3.8 Pharmacokinetics studies. The plasma concentration profiles of DTX after intravenous administration were presented in Fig. 6. The results have shown that free DTX was removed from the circulating system after 8 h. In contrast, the plasma levels of DTX in micelles systems could be remained high for a longer time. In particular, the DTX-loaded P36/TPGS MM had longest systemic circulation time and could be detected with highest plasma levels even at 24 h after administration, which exhibited drug level about 400 μg L^{-1}.

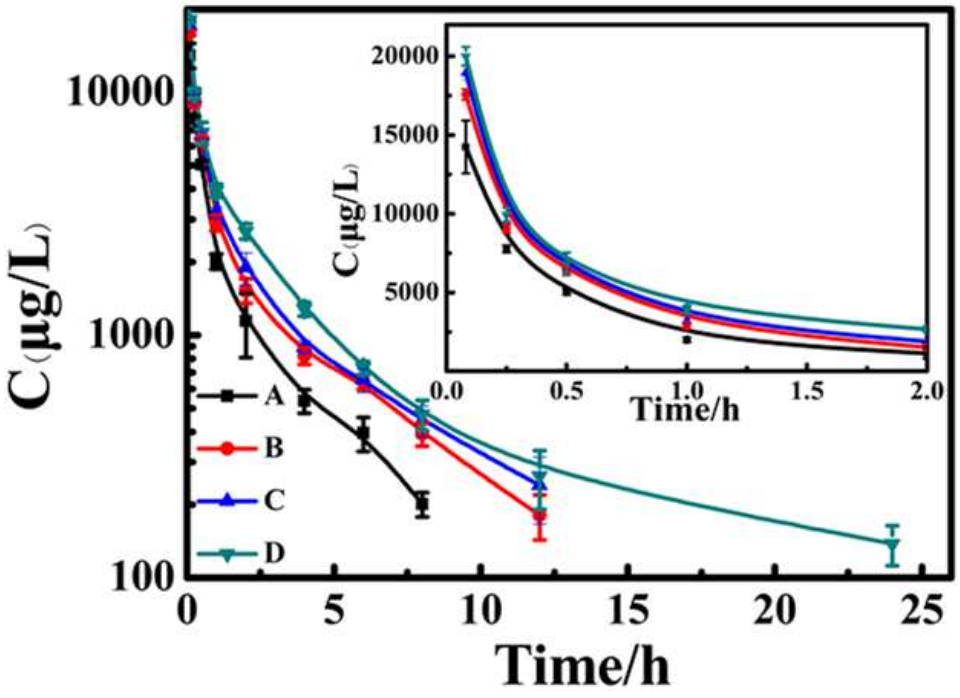

Fig. 6. Mean concentration-time curves of DTX in rat plasma after intravenous administration. (A) free DTX, (B) DTX-loaded P9/TPGS MM, (C) DTX-loaded P18/TPGS MM, (D) DTX-loaded P36/TPGS MM (mean ± SD, n=3).

The main pharmacokinetic parameters were calculated by the statistical moment method using the DAS 2.0 software (Drug and Statistics for Windows, Chinese Pharmacological Society, Shanghai, China).[39] The corresponding pharmacokinetic parameters were listed in Table 5. Statistical significance was analyzed using the student's t-test. Compared to free DTX, the DTX-loaded P9/TPGS, P18/TPGS and P36/TPGS MM formulations displayed larger $AUC_{0-\infty}$. The values of $AUC_{0-\infty}$ were 2.31-, 2.59-, and 4.63-fold compared with free DTX (260.97 μg·h mL^{-1}, 291.79 μg·h mL^{-1}, 522.53 μg·h mL^{-1} vs. 112.87 μg·h mL^{-1}), respectively. Overall, the MRT of three micelles formulations (4.15 h, 4.72 h and 10.08 h, respectively) was considerably longer (1.96-, 2.24-, and 4.78-fold, respectively) than free DTX (2.11 h). They also presented a relative longer $T_{1/2\alpha}$ (1.68-, 1.96- and 1.92-fold, respectively), much longer $T_{1/2\beta}$ (5.52-, 6.27-, and 17.17-fold, respectively) and much slower CL (1.35-, 1.49-, and 2.75-fold slower, respectively). These could be attributed to the nanosize dimension and the outmost PEO shell which could escape the reticuloendothelial system (RES) uptake and renal clearance. The prolonged circulation illustrated that PEO-PPO-PCL/TPGS MM was be able to retain a

significant proportion of loaded-DTX *in vivo* and preferentially accumulate in tumors via the EPR effect, improving the antitumor effect.

Table 5.

The pharmacokinetic parameters of four formulations after intravenous administration in rats (13 mg kg^{-1} of DTX, mean ± SD, n=3).

Formulations	$AUC_{0-\infty}$ (μg· h mL^{-1})	MRT (h)	CL (mL/ h·kg)	$T_{1/2\alpha}$ (h)	$T_{1/2\beta}$ (h)
Free DTX	112.87 ± 3.01	2.11 ± 0.09	0.88 ± 0.09	0.25 ± 0.01	0.64 ± 0.07
DTX-loaded P9/TPGS	260.97 ± 4.67*	4.15 ± 0.01*	0.65± 0.08$^{\Delta}$	0.42 ± 0.08$^{\Delta}$	3.53 ± 0.06*
DTX-loaded P18/TPGS	291.79 ± 3.90*	4.72 ± 0.04*	0.59 ± 0.06*	0.49 ± 0.12$^{\Delta}$	4.01 ± 0.16*
DTX-loaded P36/TPGS	522.53 ± 3.15*	10.08 ± 0.19*	0.38 ± 0.03*	0.48 ± 0.05$^{\Delta}$	10.99 ± 0.09*

Note: $T_{1/2\alpha}$, the distribution half life $T_{1/2\beta}$, the elimination half life $AUC_{0-\infty}$, the area under plasma concentration–time curve to time infinity CL, plasma elimination rate MRT, mean residence time * $P < 0.01$ compared with free DTX Δ $P < 0.05$ compared with free DTX.

3.9 Inhibition of P-gp efflux assay in MCF-7/Adr cells. It has been proved that TPGS could inhibit P-gp even at low concentrations.[40] Therefore, TPGS released from the mixed micelles may also help to inhibit P-gp. A study was conducted in P-gp overexpressing MCF-7/Adr cells using RH123 as P-gp marker substrate. Cell accumulation of RH123 with Vrp (P-gp efflux inhibitor) treatment was applied as positive control. As could be seen from Fig. 7, the accumulation of RH123 in cells treated with TPGS-micelles was similar with that in cells treated with free TPGS. However, the cells treated with TPGS and TPGS-micelles showed more RH123 accumulation than those treated with non-TPGS-micelles. The quantitative data showed that the cells treated with TPGS and TPGS-micelles were about 3-fold higher RH123 accumulation than those treated with non-TPGS-micelles, which indicated that TPGS could markedly increase RH123 accumulation in MCF-7/Adr cells.

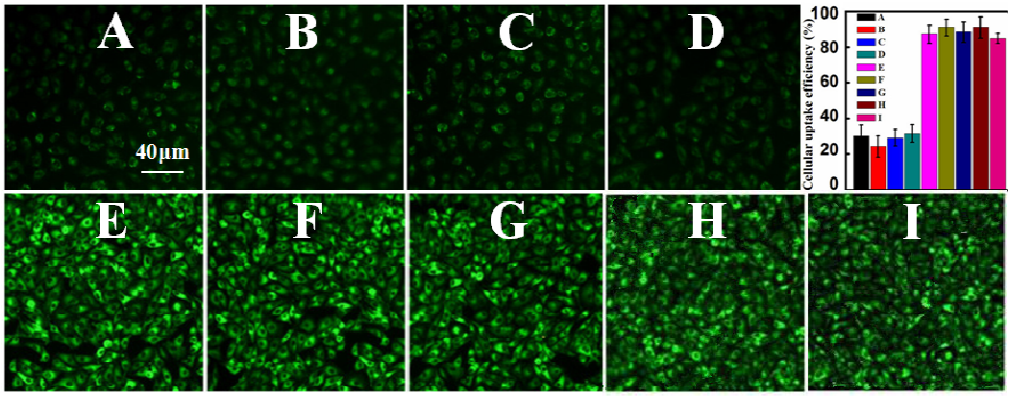

Fig. 7. P-gp inhibition assay of RH123 intracellular accumulation in MCF-7/Adr cells that were (A) untreated and treated with (B) blank P9 micelles, (C) blank P18 micelles, (D) blank P36 micelles, (E) Vrp, (F) TPGS, (G) blank P9/TPGS micelles, (H) blank P18/TPGS micelles, (I) blank P36/TPGS micelles (mean ± SD, n=6).

3.10 The cellular uptake of C6-loaded non-TPGS micelles and TPGS-micelles in MCF -7/Adr cells. Cellular uptake is the key step for drug to fulfill their anticancer activity. To further investigate whether the addition of TPGS in micelles could increase the cellular uptake, the cellular uptake assay were carried out on P-gp overexpressing MCF-7/Adr cells. The sizes of DTX-loaded micelles and the corresponding C6-loaded micelles were similar (Fig. S1), therefore, C6-loaded micelles could be used as a substitute of DTX-loaded micelles for cellular uptake experiments. It should be noticed that C6-loaded TPGS-participating micelles showed an obvious higher accumulation in MCF -7/Adr cells than non-TPGS micelles after 8 h incubation (Fig. 8). The increased cellular uptakes of TPGS-participating micelles were resulted from the TPGS-induced P-gp inhibition. Therefore, the TPGS-participating micelles had much more advantages in cell uptake over the non-TPGS micelles.

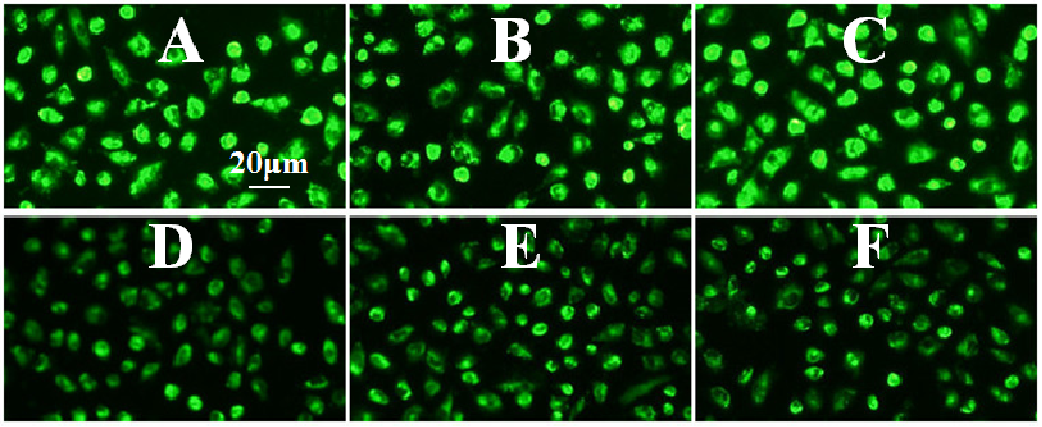

Fig. 8. Fluorescent micrographs of MCF-7/Adr cells incubated for 8 h in different samples (A) C6-loaded P9/TPGS MM, (B) C6-loaded P18/TPGS MM, (C) C6-loaded P36/TPGS MM, (D) C6-loaded P9 micelles, (E) C6-loaded P9 micelles, (F) C6-loaded P36 micelles.

3.11 The cellular uptake studies and flow cytometric (FCM) analysis. In order to investigate the cellular uptake, coumarin-6 (C6) is used as a model fluorescent molecule to represent DTX, because its fluorescence enables easy quantitative and qualitative analysis. Fig. 9 and Fig. S2 displayed MCF-7 and A549 cells after incubation with different C6 formulations. Fluorescence microscopy images (Fig. 9 I and Fig. S2 I) showed the internalization of C6 or C6-loaded MM in cells. For cells treated with free C6, the lower intracellular fluorescence intensity was observed both in MCF-7 and A549 cells, demonstrating that it was relatively difficult for C6 molecule alone to penetrate the cell membrane. The micelles play an important role in mediating intracellular uptake. The presence of PEO shell on the surface of micelles which favors direct interaction with cells resulting in enhanced uptake mediated through endocytosis.[41] In the first two hours, C6-loaded MM were localized extensively in the cytoplasmic region. With longer incubation time, the fluorescence became stronger, and more fluorescence could be observed in cell nucleus. The quantitative data from the flow cytometry assay for MCF-7 and A549 cells were shown in Fig. 9 II and Fig. S2 II, the untreated cells were used as a control to show the autofluorescence. It is clear that the fluorescence of cells treated with C6-loaded MM showed an obvious higher accumulation than free C6, approximately 3-9 times the intensity (Fig. 9 III and Fig. S2 III). On the whole, cellular uptake showed a faster and more accumulation of the micelles within tumor cells than free drug. This is

because free C6 molecules and C6-loaded mixed micelles have different ways to enter cells. C6 molecule is transported by diffusion mechanisms, affected by P-gp efflux pumps. Whereas the C6-loaded micelles provide an alternative route of internalization via the endosomal pathway, which is speculated to be a major course for nanoparticles to circumvent drug reflux mechanisms associated with MDR.[42]

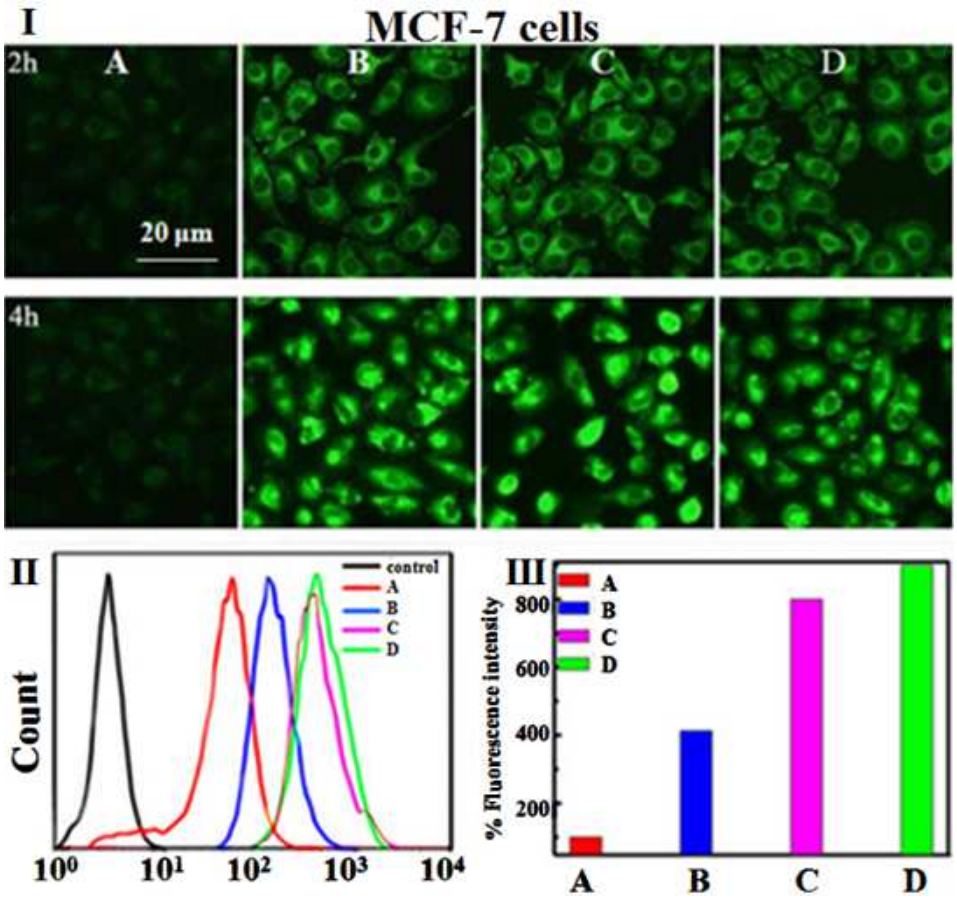

Fig. 9. Fluorescent micrographs (I, for 2h and 4h), flow cytometric profiles of intensity (II) and corresponding quantitative histogram profiles (III) of MCF-7 cells incubated for 4 h in different samples. (A) free C6, (B) C6-loaded P9/TPGS MM, (C) C6-loaded P18/TPGS MM, (D) C6-loaded P36/TPGS MM. The fluorescence intensity of free C6 was expressed as 100%.

3.12 Cytotoxicity assay. *In vitro* cytotoxicity of blank MM and DTX-loaded MM were evaluated by MTT assays. Herein, MCF-7 and A549 cells were respectively co-cultured with different samples at various concentrations for 24 h, 48 h and 72 h. As revealed in Fig. S3, the blank MM had no apparent cytotoxicity on the growth of the two studied cells. Hence, the blank MM are expected to be safe for biomedical

applications. The results of cytotoxicity of DTX-loaded MM were indicated in Fig. 10. A time-dependent and dose-dependent cytotoxicity were observed. It is straightforward to understand that the higher cytotoxicity is achieved by both higher concentration and longer incubation time. More DTX have been released from the micelles and thus available to exert its cytotoxic activity after longer incubation periods. Besides, larger numbers of cells entered G2 and M cell cycle phases, where DTX selectively induced polymerization of tubulin monomer and inhibits depolymerization leading to mitotic arrest.[43] On the other hand, larger amounts of TPGS released from the micelles, preventing DTX from being pumped out of the cell by P-gp and have synergistic anticancer activity. On the whole, the results clearly indicated that the DTX-loaded TPGS-participating MM was very effective in inhibiting the growth of both MCF-7 and A549 cells. The micelles were taken up by cells through an endocytosis pathway, which escapes the pumping-out action of P-gp, thereby resulting in a higher intracellular drug concentration. However, free DTX enters cells by passive diffusion mechanism, a P-gp-dependent pathway, thus smaller numbers of DTX molecules accumulate in cells.

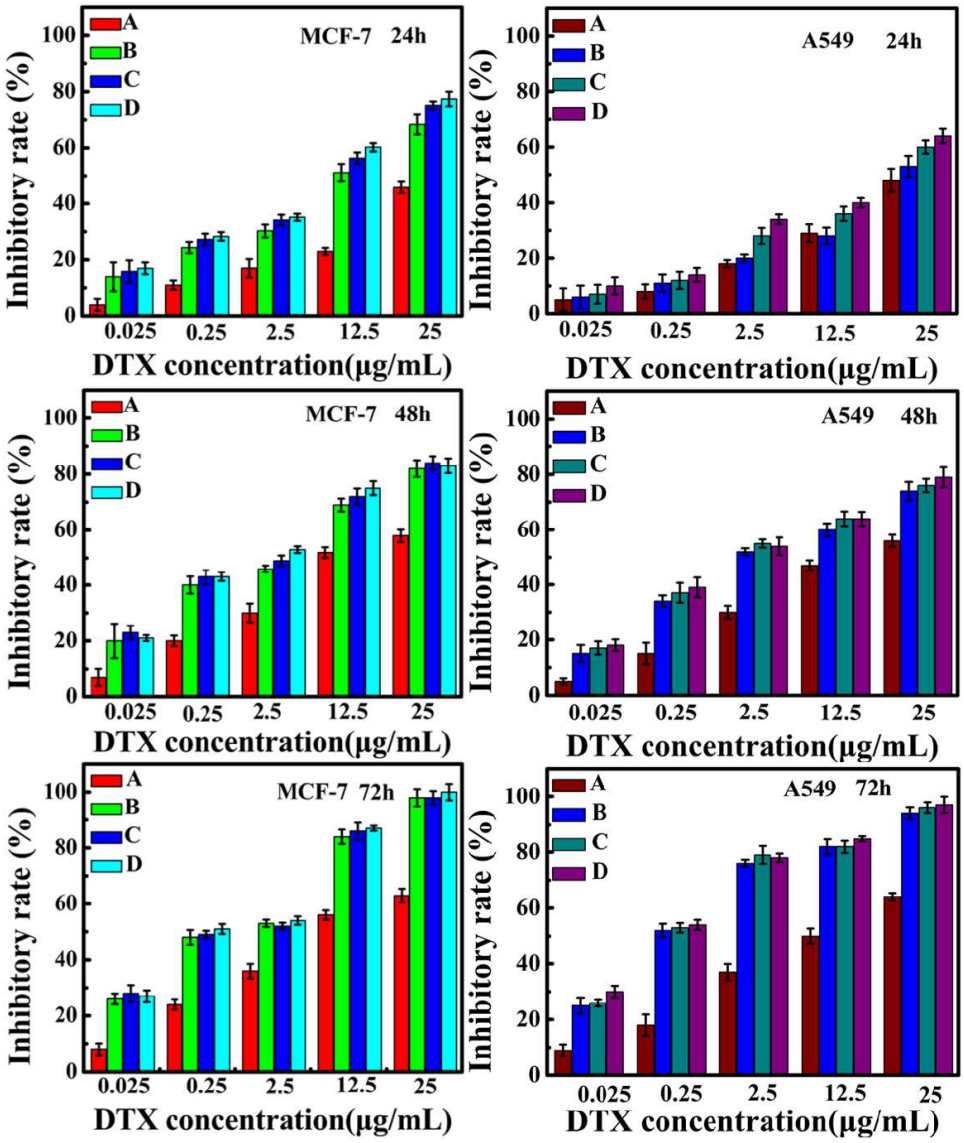

Fig. 10. Cytotoxicity study of DTX-loaded MM and free DTX in A549 cells and MCF-7 cells for 24 h, 48 h and 72 h. (A) free DTX, (B) DTX-loaded P9/TPGS MM, (C) DTX-loaded P18/TPGS MM, (D) DTX-loaded P36/TPGS MM (mean ± SD, n=6).

3.13 IC50 values of DTX-loaded mixed micelles. The efficacy of killing tumor cells by different formulations could be further quantitatively demonstrated by the IC50 value (drug concentrations that kill 50% of cells). The IC50 values of MCF-7 and A549 cells incubated with different DTX formulations for 24, 48 and 72 h were listed in Table 6. These results were in good agreement with the above cell cytotoxicity results. Overall, in both cell lines, DTX formulations inhibited cells growth in a time-dependent manner. The IC50 of DTX-loaded MM was lower than that of free DTX at different time. It was particularly worth mentioning that, P9/TPGS MM, P18/TPGS

MM and P36/TPGS MM illustrated a 69-, 82-, and 100-times lower IC50 value compared with free DTX, respectively, after 72 h incubation in MCF-7 cells. The IC50 values demonstrated that three DTX-loaded MM could be 11-, 12- and 23-fold more effective than free DTX, respectively, after 72 h treatment with A549 cells. What's more, we noticed that the cytotoxicity of the same formulation was different between the two cell lines. All the formulations showed stronger effect on killing MCF-7 cells than A549 cells, which attributed to the differences in their biological behaviors and genetic background. The difference of intracellular esterase activities between the two cell lines may also contribute to the different levels of cytotoxicity.

Table 6.

IC50 values of different formulations after incubation with MCF-7 and A549 cells for 24 h, 48 h and 72 h (mean ± SD, n=6).

Formulations	IC50 (μg mL^{-1})		
	24 h	48 h	72 h
(A)MCF -7 cells			
Free DTX	22.73 ± 0.37	14.05 ± 0.56	9.01 ± 0.32
DTX-loaded P9/TPGS MM	15.23 ± 0.42$^{\Delta}$	1.56 ± 0.33*	0.11 ± 0.26*
DTX-loaded P18/TPGS MM	13.54 ± 0.89*	1.23 ± 0.54*	0.13 ± 0.19*
DTX-loaded P36/TPGS MM	12.59 ± 0.82*	1.19 ± 0.37*	0.09 ± 0.07*
(B)A549 cells			
Free DTX	31.80 ± 0.58	18.30 ± 0.54	12.75± 0.48
DTX-loaded P9/TPGS MM	20.92 ± 0.65*	2.97 ± 0.85*	1.16 ± 0.37*
DTX-loaded P18/TPGS MM	20.32 ± 0.62*	2.43 ± 0.45*	1.08 ± 0.26*
DTX-loaded P36/TPGS MM	18.14 ± 0.12*	2.29 ± 0.32*	0.56 ± 0.13*

* $P < 0.01$ compared with free DTX, Δ $P < 0.05$ compared with free DTX.

3.14 Drug induced morphology changes and PI staining. The morphology changes of cells after treated with different DTX formulations were investigated. As seen in Fig. S4, control cells and drug treatment cells showed obvious differences in both morphology and quantity. Control cells had normal morphology and grew well. However, after incubated with different DTX formulations, the number of cells declines and the morphological changes of cells could be observed. The cells have become shrinked and arranged loosely. What't more, the cellular skeletons were not

evident as the control cells. It also could be seen that the cells exposed to DTX-loaded MM have more obvious changes on morphology and more cell death than that those exposed to free DTX solution.

Propidium iodide (PI) staining is based on the principle that PI can selectively cross the membrane of apoptotic cells. Staining the damaged cells with PI is further carried out to study cells toxicity. The stained cells give red fluorescence and the strength of cell toxicity can be assessed by the increase of PI stained cells.[44] As seen in Fig. 11, control cells showed almost no red fluorescence, indicating that cells grew normally. While MCF-7 and A549 cells treated with different DTX formulations showed obvious red fluorescence, which confirmed that DTX was able to destroy the cell membrane integrity, induce the change of membrane permeability and cause the cell cytoclasis. Overall, the cell growth inhibition effect is enhanced with increase of incubation time. What's more, it was noticed that both MCF-7 and A549 cells treated with DTX-loaded MM showed more numbers of PI stained cells than those treated with free DTX solution. The DTX-loaded MM could promote apoptosis of the tumor cells ascribed to the more efficient cell uptake of the mixed micelles.

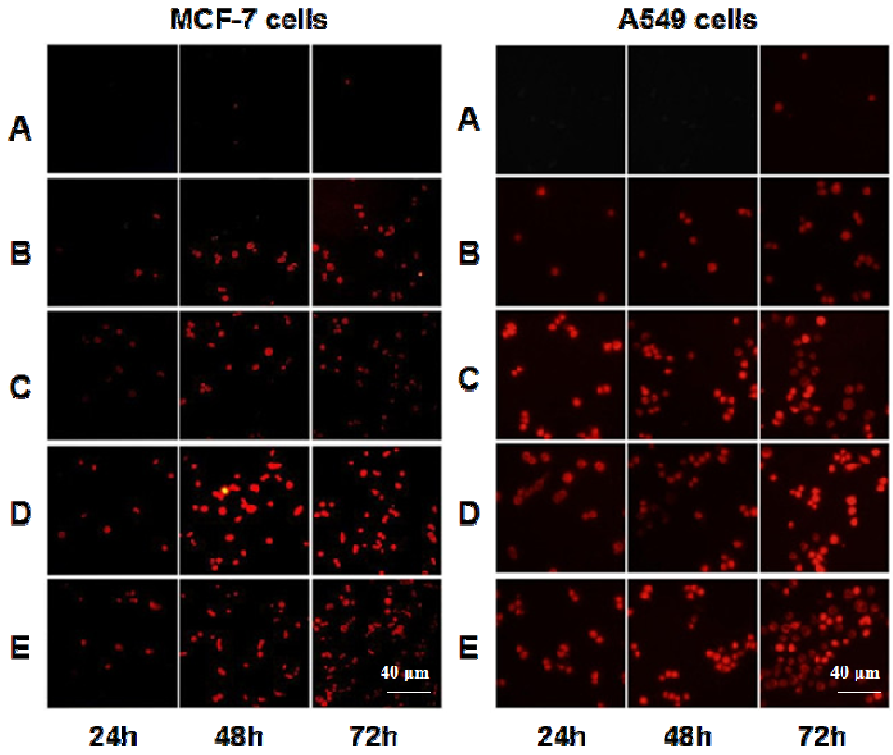

Fig. 11. PI staining images. (A) control cells, (B) free DTX, (C) DTX-loaded P9/TPGS MM, (D) DTX-loaded P18/TPGS MM, (E) DTX-loaded P36/TPGS MM.

4. Conclusions

Three series of triblock polymer PEO–PPO–PCL with different PCL molecular weight were synthesized and characterized. In present study, we have used the synthesized copolymers and TPGS to construct the mixed micelles for loading the anticancer drug DTX. The DTX-loaded mixed micelles had higher encapsulation efficiency and drug loading than those of corresponding PEO-PPO-PCL singular micelles. All the three samples could form into spherical micelles and the sizes of the mixed micelles are about 25 nm, 35 nm and 135 nm for DTX-loaded P9/TPGS MM, P18/TPGS MM and P36/TPGS MM, respectively. An obvious sustained release behavior *in vitro* was observed in DTX-loaded MM formulations and the DTX-loaded MM exhibited longer circulation time than free DTX *in vivo*. Importantly, the PEO-PPO-PCL/TPGS MM could get higher cellular uptake and significantly increased *in vitro* cytotoxicity compared with free DTX. Therefore, the prepared DTX-loaded TPGS-participating mixed polymeric micelle is a desirable drug delivery system for efficient cancer therapy.

Acknowledgements

We gratefully acknowledge financial support from National Natural Science Foundation of China (NSFC, No. 21373126), the Project-sponsored by SRF for ROCS (State Education Ministry) and Qingdao science and technology plan projects (14-2-4-7-jch).

References

1 A. Singh, M. Talekar, T. H. Tran, A. Samanta, R. Sundaram and M. Amiji, *J. Mater. Chem. B*, 2014, **2**, 8069–8084.

2 M. Xu, J. Qian, A. Suo, N. Cui, Y. Yao, W. Xu, and H. Wang, *J. Mater. Chem. B,* 2015, **3**, 2215-2228.

3 M. Sanson, M. Napolitano, R. Yaya, F. Keime-Guibert, P. Broët, K. Hoang-Xuan and J. Y. Delattre, *J. Neurooncol* ,2000, **50**, 245-249.

4 P. Forsyth, G. Cairncross, D. Stewart, M. Goodyear, N. Wainman and E. Eisenhauer, *Invest. New Drugs*, 1996, **14**, 203-206.

5 Y. C. Ma, J. X. Wang, W. Tao, H. S. Qian and X. Z. Yang, *ACS Appl. Mater. Interfaces*, 2014, **6**, 16174-16181.

6 Y. Mo, H. Wang, J. Liu, Y. Lan, R. Guo, Y. Zhang and Y. Zhang, *J. Mater. Chem. B*, 2015, **3**, 1846-1855.

7 B. T. Luk and L. Zhang, *ACS Appl. Mater. Interfaces,* 2014, **6**, 21859-21873.

8 Y. Wang, Q. Luo, R. Sun, G. Zha, X. Li, Z. Shen, and W. Zhu, *J. Mater. Chem. B*, 2014, **2**, 7612-7619.

9 C. Y. Sun, Y. C. Ma, Z. Y. Cao, D. D. Li, F. Fan, J. X. Wang, W. Tao and X. Z. Yang, *ACS Appl. Mater. Interfaces,* 2014, **6**, 22709 −22718.

10 C. Giacomelli, V. Schmidt, K. Aissou and R. Borsali, *Langmuir*, 2010, **26**, 15734-15744.

11 J. Chen, J. Ouyang, J. Kong, W. Zhong and M. M. Xing, *ACS Appl. Mater. Interfaces*, 2013, **5**, 3108-3117.

12 S. Y. Lee, S. Kim, J.Y. Tyler, K. Park and J. X. Cheng, *Biomaterials,* 2013, **34**, 552-561.

13 C. Tan, Y. Wang, W. Fan, *Pharmaceutics*, 2013, **5**, 201-219.

14 A. B. Ebrahim Attia, Z. Y.Ong, J. L. Hedrick, P. P. Lee and P. L. R. Ee, *Curr. Opin. Colloid In.*, 2011, **16**, 182-194.

15 E. S. Lee, Z. Gao, D. Kim, K. Park, I. C. Kwon and Y. H. Bae, *J. Control. Release*, 2008, **129**, 228–36.

16 L. Mu, T. A. Elbayoumi and V. P. Torchilin, *Int. J. Pharm.*, 2005, **306**, 142–149.

17 C. L. Lo, C. K. Huang, K. M. Lin and G. H. Hsiue, *Biomaterials*, 2007, **28**, 1225–1235.

18 L. Xu, Z. Zhang, F. Wang, D. Xie, S. Yang, T. Wang, L. Feng and C. Chu, *J. Colloid Interface Sci.*, 2013, **393**, 174-181.

19 Q. Liu, J. Chen and J. Du, *Biomacromolecules*, 2014, **15**, 3072-3082.

20 Y. Guo, M. Chu, S. Tan, S. Zhao, H. Liu, B. O. Otieno, X. Yang and C. Xu, *Mol. Pharm.*, 2013, **11**, 59-70.

21 C. Li, J. Jin, J. Liu, X. Xu and J. Yin, *ACS Appl. Mater. Interfaces*, 2014, **6**, 13956-13967.

22 J. Wang, J. Sun, Q. Chen, Y. Gao, L. Li, H. Li, D. Leng, Y. Wang, Y. Sun and Y. Jing, *Biomaterials*, 2012, **33**, 6877–6888.

23 J. Neuzil, J. C. Dyason, R. Freeman, L. F. Dong, L. Prochazka, X. F.Wang,

I. Scheffler and S. J. Ralph, J. *Bioenerg Biomembr*, 2007, **39**, 65-72.

24 Y. Zhu, F. Wang, C. Zhang and J. Du, *ACS nano*, 2014, **8,** 6644-6654.

25 G. H. Li and C. G. Cho, *Korean J. Chem. Eng*., 2008, **25**, 1444-1447.

26 Q. Liu, S. Chen, J. Chen and J. Du, *Macromolecules*, 2015, **48**, 739–749.

27 M. Li, W. Song, Z. Tang, S. Lv, L. Lin, H. Sun, Q. Li, Y. Yang, H. Hong and X. Chen, *ACS Appl. Mater. Interfaces*, 2013, **5**, 1781-1792.

28 H. Zhu, H. Chen, X. Zeng, Z. Wang, X. Zhang, Y. Wu, Y. Gao, J. Zhang, K. Liu and R. Liu, *Biomaterials*, 2014, **35**, 2391–2400.

29 A. B. E. Attia, Z. Y. Ong, J. L. Hedrick, P. P. Lee, P. L. R. Ee, P. T. Hammond and Y. Y. Yang, *Curr. Opin. Colloid In.*, 2011, **16**,182-194.

30 D. J. A. Crommelin, G. Storm, W. Jiskoot, R. Stenekes, E. Mastrobattista and W. E. Hennink, *J. Control. Release*, 2003, **87**, 81-88.

31 H. Maeda, J. Fang, T. Inutsuka and Y. Kitamoto, *Int. J. Immunopharmacology* 2003, **3**, 319-328.

32 M. El-Sayed, M. F. Kiani, M. D. Naimark, A. H. Hikal and H. Ghandehari, *Pharm. Res.*, 2001, **18**, 23-28.

33 R. Nahire, M. K. Haldar, S. Paul, A. H. Ambre, V. Meghnani, B. Layek, K. S. Katti, K. N. Gange, J. Singh and K. Sarkar, *Biomaterials*, 2014, **35**, 6482-6497.

34 S. Wang, S. Zhang, J. Liu, Z. Liu, L. Su, H. Wang and J. Chang, *ACS Appl. Mater. Interfaces*, 2014, **6**, 10706-10713.

35 Y. Y. Won, A. K. Brannan, H. T. Davis and F. S. Bates, *J. Phys. Chem B.*, 2002, **106**, 3354-3364.

36 C. de las Heras Alarcón, S. Pennadam and C. Alexander, *Chem. Soc. Rev.*, 2005, **34**, 276-285.

37 J. Gao, J. Ming, B. He, Y. Fan, Z. Gu and X. Zhang, *Eur. J. Pharm. Sci.*, 2008, **34**, 85-93.

38 K. Rajagopal, A. Mahmud, D. A. Christian, J. D. Pajerowski, A. E. Brown, S. M. Loverde and D. E. Discher, *Macromolecules*, 2010, **43**, 9736-9746.

39 L. Wang, Z. Liu, D. Liu, Z. Juan and N. Zhang, *Int. J. Pharm.*, 2011, **413**, 194-201.

40 H. Z. Zhao and L. Y. L. Yung, *J. Biomed. Mater. Res. A*, 2009, **91**, 505-518.

41 L. Xiao, X. Xiong, X. Sun, Y. Zhu, H. Yang, H. Chen, L. Gan, H. Xu and X.Yang, *Biomaterials*, 2011, **32**, 5148-5157.

42 B. Pavan, G. Paganetto, D. Rossi and A. Dalpiaz, *Drug Discov. Today*, 2014, **19**, 1563-1571.

43 P. Aggarwal, J. B. Hall, C. B. McLeland, M. A. Dobrovolskaia and S. E. McNeil, *Adv. Drug Deliv. Rev.*, 2009, **61**, 428-437.

44 L. Qi, Y. Guo, J. Luan, D. Zhang, Z. Zhao and Y. Luan, *J. Mater. Chem. B*, 2014, **2**, 8361-8.

Graphical Abstract

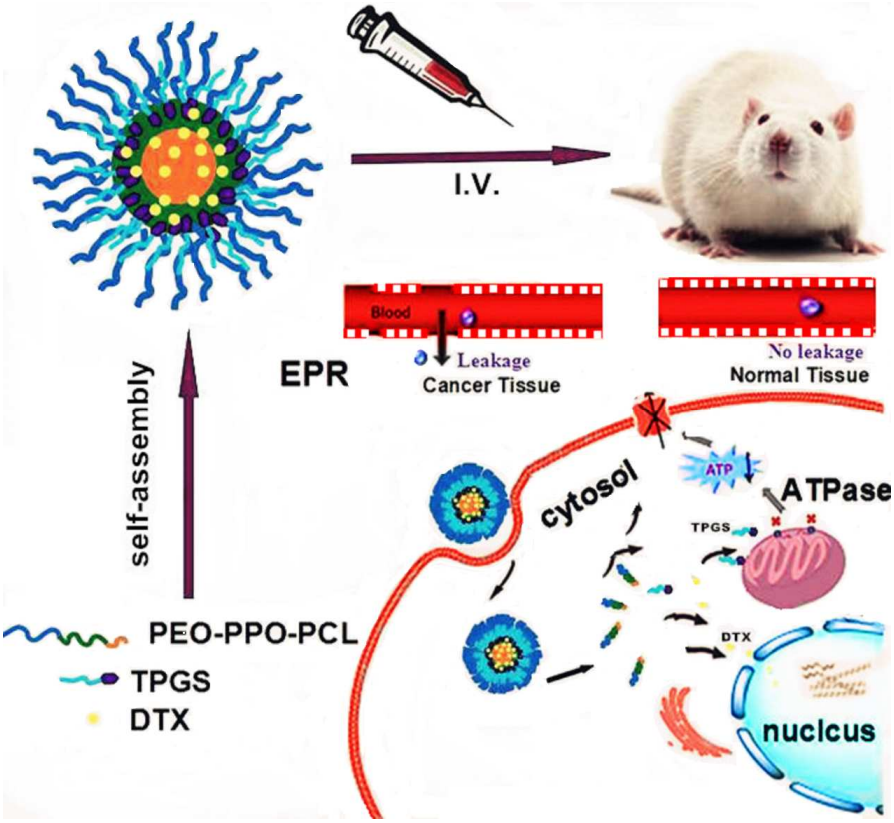

Schematic diagram of DTX-loaded PEO–PPO–PCL/TPGS mixed micelles in vivo for overcoming multidrug resistance and enhancing antitumor efficacy